



Experimental results on the performance of cryogenic treatment of tool and minimum quantity lubrication for machinability improvement in the turning of Inconel 718

Yogesh V. Deshpande^{1,2} · Atul B. Andhare² · Pramod M. Padole²

Received: 26 May 2017 / Accepted: 5 December 2017 / Published online: 3 January 2018
© The Brazilian Society of Mechanical Sciences and Engineering 2018

Abstract

Inconel 718 is a popular, but difficult to machine, nickel-based super alloy. Machining performance of this material can be improved by appropriate modelling and optimization. In the present study, response surface modelling and optimization for turning of Inconel 718 under four machining conditions: dry with untreated inserts, dry with cryogenically treated inserts, minimum quantity lubrication with untreated inserts and minimum quantity lubrication with cryogenically treated inserts is carried out. With the aim of improving the machinability of Inconel 718, an attempt has been made to examine the effect of cryogenic treatment of tool and minimum quantity lubrication in terms of indicators such as surface quality of workpiece, tool wear and material removal rate. Cutting speed, feed rate and depth of cut are used as the control parameters. Whereas, cutting force, tool vibration, cutting temperature, surface roughness and tool wear are the measured responses. Prediction models are developed for each response. Later, all the responses are optimized together by desirability approach and are validated using confirmation experiments. A spider plot is drawn to display the relationships among control and response parameters. The plot shows that application of minimum quantity lubrication with cryogenically treated inserts resulted in least cutting force, tool vibration, cutting temperature, minimum surface roughness of workpiece along with least tool wear and best material removal rate compared to other three conditions used. This clearly shows machinability improvement of Inconel 718.

Keywords Cryogenic treatment · Inconel 718 · Minimum quantity lubrication · Response surface methodology · Surface roughness

Abbreviations

ANOVA	Analysis of variance
CCD	Central composite design
CNC	Computer numerical control
DRY	Dry cutting with untreated carbide inserts

DRY-CT	Dry cutting with cryogenically treated inserts
MQL	Minimum quantity lubrication with untreated inserts
MQL-CT	Minimum quantity lubrication with cryogenically treated inserts
RSM	Response surface methodology
SEM	Scanning electron microscope
VHN	Vickers hardness number

Technical Editor: Márcio Bacci da Silva.

✉ Yogesh V. Deshpande
deshpande_yv@yahoo.co.in; deshpadeyv@rknec.edu

Atul B. Andhare
abandhare@mec.vnit.ac.in

Pramod M. Padole
pmpadole@rediffmail.com

¹ Shri Ramdeobaba College of Engineering and Management, Nagpur 440013, India

² Department of Mechanical Engineering, Visvesvaraya National Institute of Technology, Nagpur 440010, India

List of symbols

A_s	Tool vibration (acceleration), g
α	Tungsten carbide phase
β	Cobalt binder phase
D	Overall desirability objective function
DCT	Deep cryogenic temperature, °C
d_i	Individual desirability values
d	Depth of cut, mm
F_c	Cutting force, N
f	Feed rate, mm/rev

MAE	Mean absolute error, %
MRR	Material removal rate, mm ³ /min
R^2	Correlation coefficient
R_a	Surface roughness, μm
T	Cutting temperature, K
VB_{max}	Tool flank wear at nose region, mm
v	Cutting speed, m/min
γ	Gamma phase
γ'	Gamma prime phase

1 Introduction

Machining processes are one of the important manufacturing activities contributing to the growth of global economy [1]. Inconel 718 (nickel-based super alloy) is having diverse applications in marine, aerospace, petroleum, food processing industries, etc. due to its properties such as high strength, high hot hardness, high impact strength, and corrosion resistance [2–4]. These properties along with work hardening tendency, poor thermal conductivity (11.2 W/mK) [5, 6] and tendency to form a built up edge pose difficulties in machining. Machining of Inconel is associated with high value of cutting forces resulting in higher vibrations and poor surface finish of the work piece. Also, low thermal conductivity of the material causes more heat transfer to the tool resulting in rise of tool temperature [7] and accelerated wear of the tool. The selection of the cutting parameters and cutting fluid is an inseparable part in any machining process [8] and it is much more important in machining of difficult-to-cut material such as Inconel 718.

Surface roughness investigation plays an important role in controlling friction, wear and fatigue of the machined parts [9] and thus it is an important response to be measured. Surface finish in machining depends upon the machine tool, cutting process, cutting parameters, cutting fluid, tool and work piece material [10]. Turning is fundamental manufacturing operation and it is imperative that the selection of appropriate cutting tool, cutting fluid and the method of application of cutting fluid plays a crucial role in turning. The investigation of cutting forces is critical as it affects the surface finish of the work piece and wear of the tool.

Selection of cutting fluid and the method of its application is one of the important parameters that affect the quality of work part. Selecting right kind of cutting fluid ensures improved quality of the surface by avoiding the overheating of the cutting zone, arresting the heat transfer to adjacent machining zone and conveying the chips away from the machining area [11]. Water-based flood cooling is a cheap, popular and prevalent method in machining. However, major disadvantage of water-based fluid is that it can propagate the growth of microorganisms in all spaces

of machine tool. Antibacterial agents which are added to fluids to reduce the growth of microorganisms get in contact with high temperature machined surface and liberate gases that are harmful to the machinist's health. Second, the repeated use of the cutting fluid alters its chemical and physical properties which may be detrimental to machining process [11, 12]. The usage of water-based fluid is also marred by low viscosity index, inadequate thermal stability and cooling capacity, thereby rendering them ineffective for the machining of Inconel.

Biodegradable vegetable oils are popular choice over the water-based fluids as they retain their properties at elevated temperature. Davoodi and Tazehkandi [13] used biodegradable vegetable oil as a cutting fluid in turning of Inconel 738. They developed empirical models using analysis of variance (ANOVA) and optimized the cutting parameters using response surface methodology (RSM). However, these cutting fluids are still not popular on account of their high cost. The quantity of the vegetable oil used for the machining can be reduced using it with minimum quantity lubrication (MQL) approach [11]. In view of all the issues discussed above, it is very important to formulate a new approach which is sustainable and improves the machining performance [14]. The use of MQL, cryogenic cooling, cryogenic treatment (cryo treatment) of tools, tool coatings, plasma heating of work piece, etc. are some of the techniques used for improving the machining of nickel alloys. Some works reporting use of these techniques are discussed in the following paragraphs.

One of the popular cryogenic techniques is use of cryogen such as liquid Nitrogen for cooling. Pusavec et al. [1, 15] have developed performance-based models for estimating tool wear, cutting forces and surface roughness using ANOVA for machining of Inconel 718. They evaluated the combined effect of cryogenic cooling with MQL and optimized the machining parameters. It was found that cryogenic cooling enhanced the quality of the machined surface compared to other conditions. Kaynak [16] had also used cryogenic cooling for turning of Inconel 718 and compared the results with those of dry and MQL conditions. MQL conditions demonstrated significant reduction in cutting forces compared to dry and cryogenic cooling at low speeds of about 60 m/min.

Cryogenic treatment of tools is also used for improving machining. It alters the metallurgical properties of tools material [17, 18] that result in improved mechanical properties. Gill et al. [19] have used cryogenically treated (cryo-treated) tungsten carbide inserts in turning of steels. They reported better wear resistance, tool life, cutting forces and surface roughness while using cryo-treated inserts compared to untreated inserts. Gill et al. [20] also reported better performance of cryo-treated tool in wet condition compared to dry machining. This is quite natural

as cutting fluid provides cooling and lubrication resulting in reduced cutting forces, temperature, tool wear and surface roughness. Thakur et al. [6] have proposed a regression equation for tool life and degree of work hardening for machining of Inconel 718 using cryo-treated tools. They observed minimum work hardening, tool wear and cutting forces while using cryo-treated tool. Deshpande et al. [21] have established regression models using RSM for estimating surface roughness with untreated and cryogenically treated inserts in turning of Inconel 718.

Another method which is attempted by some researchers, to improve machining, is hybrid machining. In this method, work piece is softened by laser or plasma heating and at the same time cryogenic cooling by liquid nitrogen (LN_2) is also used at the chip tool interface to carry away the heat produced in machining region. Researchers have reported reduction in cutting forces, tool wear and surface roughness in hybrid machining of Inconel 718 compared to conventional machining. As reported by Feyzi and Safavi [22], there was no change in the hardness of the machined surface in hybrid machining. Few researchers have attempted dry machining of nickel-based alloys using integrated optimization techniques discussed in the following paragraphs.

Pawade and Joshi [23] had performed dry turning operation on Inconel 718 using CBN insert. The optimum cutting parameters were found out using Taguchi grey relation analysis for minimizing cutting forces and surface roughness. Homami et al. [24] performed dry turning of Inconel 718 with coated insert. Cutting speed, feed rate, nose radius and approach angle were selected as cutting parameters. ANOVA and genetic algorithm approach were used to find the optimum cutting condition for achieving minimum surface roughness and flank wear. For achieving good surface quality of Inconel 825 (nickel-based alloy) in minimum time, Tamang and Chandrasekaran [25] combined ANN model with particle swarm optimization (PSO) and optimized machining parameters in dry turning of Inconel 825 using polycrystalline diamond (PCD) inserts.

From the various works discussed above, it is seen that dry machining with uncoated tool is not suitable for Inconel 718. The absence of coolant and lower thermal conductivity of Inconel 718 results in increased heat transfer to the tool, which results in rapid tool wear. The excessive friction and higher contact between the tools and chip edge result in formation of the dull tool edge which further increases the cutting force. This is a vicious circle as blunt cutting edge increases the cutting force which in turn increases the wear. Cryogenic cooling can have adverse effect on cutting force and surface finish due to excess cooling [26, 27]. Also, the hybrid machining of nickel alloys is not economical. It is also found from literature that MQL provide better results at low cutting

speed of about 60 m/min as MQL helps in heat dissipation. However, at high speed, MQL does not give appreciable results in the machining for Inconel 718 [16]. The cryo-treated tool can bear high temperature without failing by plastic deformation [18]. The literature review reveals that use of cryogenic techniques enhance the machinability of various materials [19, 20, 28–30]. Therefore, technique of cryogenic tool treatment can also be tried for material such as Inconel 718.

From the various reported works, it is observed that there is hardly any work on machining of nickel-based super alloy using cryogenic treatment of tools and MQL approach. Thakur et al. [6] have reported the use of cryo-treated inserts for machining of Inconel 718 and this is limited to dry condition only. It is also seen that the cryogenic cycle to be used for tool treatment and the appropriate parameters required for machining of nickel alloys are required to be examined. Also, use of modelling techniques in such investigations would be beneficial for reducing the costly and time-consuming experimentation [31]. Further, using MQL with cryo-treated inserts is cheaper than using cryogenic cooling with liquid nitrogen.

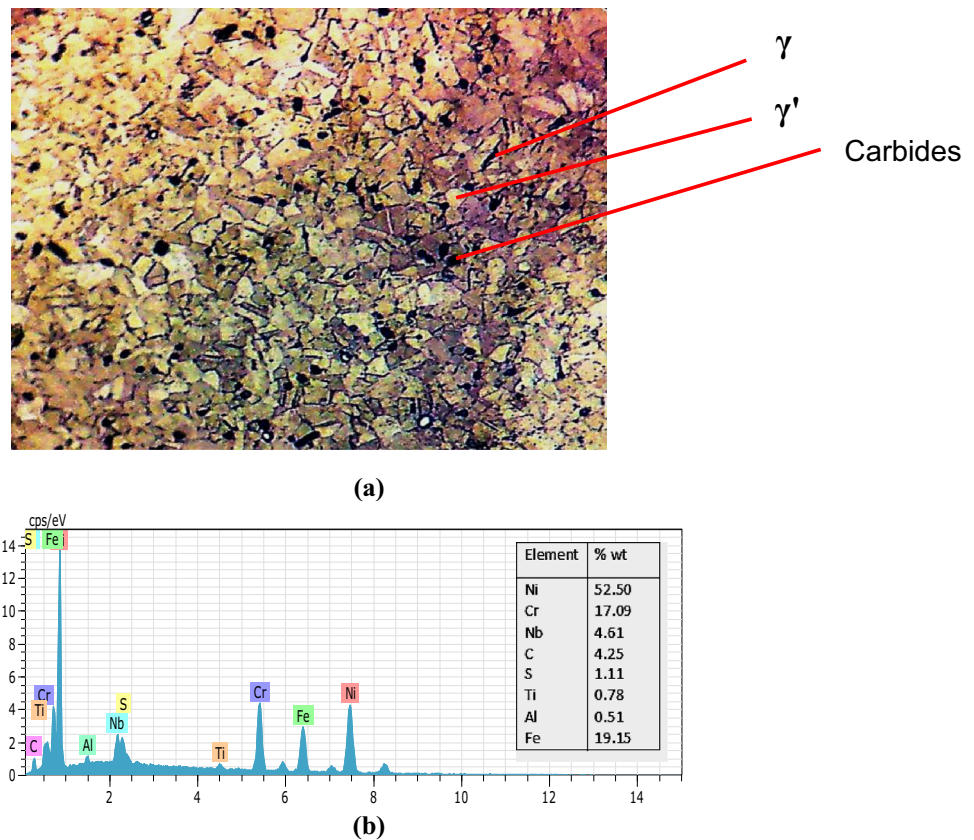
In this context, the present work deals with the novel combination of use of cryogenically treated tools with MQL condition in machining of Inconel 718. The effect of cutting parameters on responses such as cutting force, tool vibration, cutting temperature, surface roughness and tool wear is determined using different machining conditions to optimize the cutting parameters for improving the machining of Inconel 718.

2 Experimentation

2.1 Work piece and tool material

In this experimental study, bars of diameter of 22 mm and length of 150 mm of Inconel 718 having hardness 46 HRC were selected for machining. Figure 1 shows the microstructure and EDX plot with chemical composition of Inconel 718, developed by scanning electron microscope (SEM). The microstructure consists of gamma (γ), gamma prime (γ') phase, carbides and metal precipitates. Gamma phase has a continuous matrix in a face-centered cubic structure. Nickel-based phase (γ phase) consists of a high percentage of disordered elements in solid-solution which is soft and ductile in nature. Gamma prime is the main strengthening and a coherently precipitating phase in Inconel 718 having a regular crystal structure, has long time stability and is brittle in nature except at very high temperature. Along with these phases, there are various inter-metallic phases of carbide and other metals. The

Fig. 1 Inconel 718
a Microstructure and **b** EDX plot



microstructure of the nickel is strengthened by these phases [32].

Uncoated tungsten carbide inserts (Kennametal make) having ISO designation TNMG 160408 with double chip breaker geometry and nose radius of 0.8 mm were utilized for experiments. Each insert was mounted on left hand tool holder with ISO designation MTJNL2525-M16 and new cutting edge was used for every experiment. The selection of the tools, cryo treatment cycle and cutting conditions were based on the tool manufacturer's manual and references from the literature [1, 6, 33]. The details pertaining to the cutting conditions are as follows: cutting speed = 9.5–110.45 m/min, feed rate = 0.06–0.23 mm/rev and depth of cut = 0.32–1.17 mm at constant cutting length of 60 mm.

2.2 Machining conditions in turning of Inconel 718

Following are the conditions used for machining of Inconel 718 alloy.

1. Dry cutting with untreated carbide inserts (DRY).
2. Dry cutting with cryogenically treated inserts (DRY-CT).

3. Minimum quantity lubrication with untreated inserts (MQL).
4. Minimum quantity lubrication with cryogenically treated inserts (MQL-CT).

For conditions 3 and 4, cutting fluid used is BioCut 3600. The pure cutting oil is sprayed directly at cutting region with the use of minimum quantity lubrication (MQL), and single nozzle spraying system (Make: DROPCO). The coolant pressure is kept at 4 bars with flow rate of 80 mlph. Uncoated tungsten carbide inserts were treated using deep cryogenic cycle as discussed in the next section.

2.3 Cryogenic treatment for carbide inserts

From the various cryo treatment cycles used by different researchers, it is seen that treatment temperatures vary significantly from -70 to -196 °C. Also, the overall cycle time of treatment has lot of variations. The increase in the tool life, wear resistance and improved surface quality was recorded using cryo-treated inserts in different operating conditions [20, 34–36]. It is also revealed that use of deep cryogenic treatment cycle (-196 °C) can be beneficial for better wear resistance of carbide inserts and further use of tempering cycle ($+196$ °C) removes the

stresses developed in the cryogenic cycle. Hence, cooling rate of cryo treatment cycle was employed as $0.5\text{ }^{\circ}\text{C}/\text{min}$ to prevent thermal shocks from swift cooling resulting in possible damage to carbide inserts. [19, 20, 28–30].

The schematic of the cryogenic system and details of cryogenic double tempering cycle used for treatment of tool inserts are shown in Fig. 2. In the cooling cycle, temperature was controlled with the computerized temperature controller at the rate of $0.5\text{ }^{\circ}\text{C}/\text{min}$ which required 8 h to obtain $-196\text{ }^{\circ}\text{C}$ (A–B). In the soaking cycle, deep cryogenic temperature (DCT) was maintained for 24 h at the coolest temperature ($-196\text{ }^{\circ}\text{C}$) from B to C. Then, it was allowed to achieve the room temperature in 8 h which is known as the warming temperature cycle (C–D). The entire duration of the cryogenic cycle was about 40 h (A–D).

Once the cryogenic cycle was completed, the material was tempered. In tempering cycle, it was heated to $+196\text{ }^{\circ}\text{C}$ in 1 h (D–E). In holding cycle, material was maintained at the high temperature for 2 h (E–F) and then allowed to cool to room temperature in the subsequent cooling cycle (F–G). The entire length of tempering cycle (D–G) is 4 h and it was repeated (G–J) for releasing the stresses developed in the cryogenic cycle. The total duration of the cryogenic double tempering cycle is 48 h (A–J). For the present work, the cryo treatment of inserts was performed at KRYO SPACE, India.

Figures 3 and 4 show the microstructure with EDX report of the untreated and treated tungsten carbide tools, obtained by SEM. The microstructure mainly comprises of the three distinct phases, alpha (α), beta (β) and eta (η), and it is similar to that reported by researchers—Gallagher et al., Gill et al., Reddy et al. and SreeramaReddy et al. [17, 18, 28, 37]. The effects of cryo treatment on microstructure of inserts are compared using EDX report and Vickers hardness values.

For untreated inserts, rough discontinuous transfer film is present in matrix (α phase) with 89.52% of tungsten and carbide along with carbon atom (W + C). White spots (β

phase) are present in the matrix with 2.46% of cobalt binder (Co) as shown in Fig. 3. After cryogenic treatment, the α phase is evenly scattered in the β phase and shows smooth and homogenous distribution as in Fig. 4a. Here, the percentage of W + C is 96.26; thus, there is 7.52% improvement compared to untreated insert as seen through EDX plot shown in Fig. 4b. Cryo treatment also reduces the cobalt binder (Co) by 25.2%. The improvement in α and β phases help to improve the overall thermal conductivity and wear resistance thus enabling better heat dissipation compared to untreated tool. Enhanced heat transfer reduces the issue of the heat build up on the tool surface and results in reduced wear. Hence, cryo-treated tool can survive at high temperature without deteriorating by plastic deformation [18].

The η phase consists of the carbides of tungsten accompanied by at least one metal binder. This phase may appear as grey spots and scatter throughout the entire bulk of the material. The change of η phase carbides after cryo treatment was reported by Gill et al. [18]. However, in the present investigation, this phase is not distinguished clearly through SEM report. Additionally, Vickers hardness (30 kgf hardness) test is performed to confirm any improvement with these phases. Hardness measurement tests are repeated for several points. The measured values are found close to each other. Hence, the mean value of hardness in Vickers Hardness Number (VHN) is reported. These values are obtained as 1474 VHN and 1576 VHN for untreated and cryo-treated inserts, respectively. The standard deviation is evaluated from mean values and these values are found as 14.84 and 18.23 for untreated and cryo-treated inserts, respectively. The hardness of carbide insert was increased by 7% after the specimen was subjected to cryogenic double tempering cycle.

2.4 Experiment setup

Turning was carried out on MTAB CNC lathe machine (Maxturn Plus⁺) of 5.5 kW equipped with Siemen's

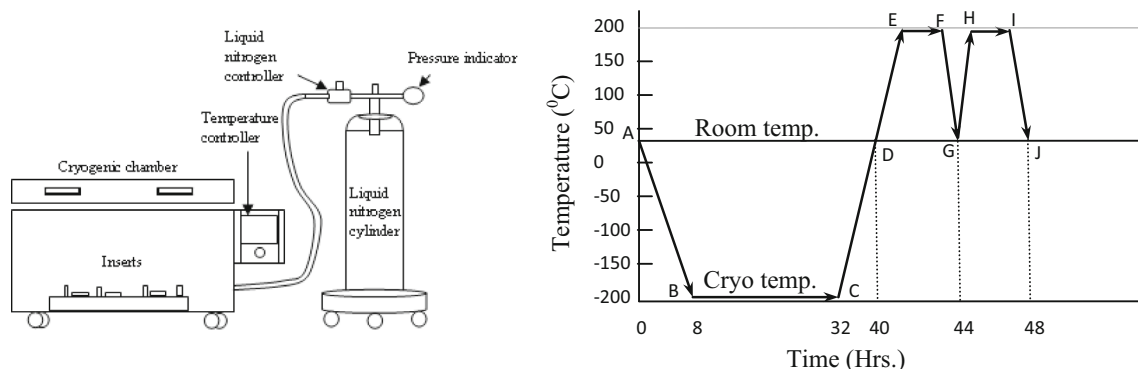
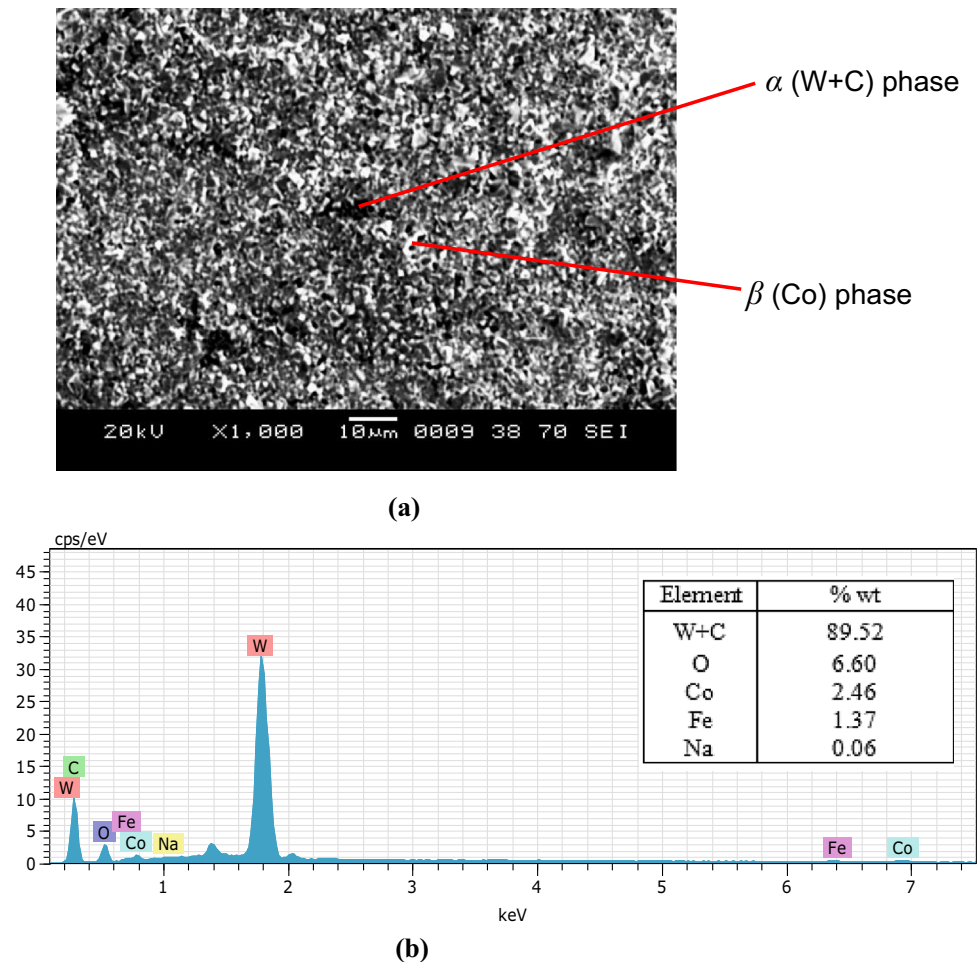


Fig. 2 Schematic of the cryogenic system (left) and deep cryogenic treatment cycle (right)

Fig. 3 Untreated carbide insert
a Microstructure, **b** EDX plot



Sinumerik 828D control. The experimental setup with measuring instruments related to turning of Inconel 718 is shown in Fig. 5. The cutting forces were measured using piezoelectric dynamometer (Make: Kistler, type: 9257B). The tool vibrations in transverse direction were measured with Industrial ICP[®] single-point accelerometer (Make: IMI sensors, model: 603C11). The output signals of dynamometer and accelerometer were acquired with National Instrument's DAQ 9178 and stored in computer using Lab VIEW 2012. After completion of all the experiments, the surface roughness values of machined parts were measured with portable surface roughness tester (Make: Mitutoyo, SURFTEST SJ-410). Surface roughness (R_a) measurements were repeated at several points on circumference of the work piece. The values were very close to each other and their average R_a is considered for further study. The tool flank wear was measured with the help of USB microscope (UM5 CAM). The values of flank wear at nose region (VB_{max}) were then noted for further analysis. The maximum temperature generated at tool-chip interface while machining was measured using a digital thermometer having range up to 1850 °C (MEXTECH IR 1800 with

thermocouple). For getting accurate temperature, K-type thermocouple probe with range up to 1370 °C is attached at a distance of 0.5 mm from the cutting edge as recommended by Tazehkandi et al. [11].

2.5 Experiment design and results

The focus of the experiments was to examine the effect of cryogenic treatment of tool and minimum quantity lubrication in turning of Inconel 718, on various responses such as cutting force, tool vibration, cutting temperature, surface roughness and tool flank wear. RSM is used for the modelling and optimization of the machining process. The experiments were designed using the central composite design (CCD) of RSM [21].

The design consists of a factorial design or corner portion (2^k) of cube, centre points and axial or star points. The corner portions of cube show eight experiments with 2^3 factorial design levels coded by -1 and $+1$, situated at the vertices of central composite design (CCD). Repetitive six experiments show an added centre point to the CCD which helps to confirm the repeatability of measuring process.

Fig. 4 Deep cryogenic treated carbide insert **a** Microstructure, **b** EDX plot

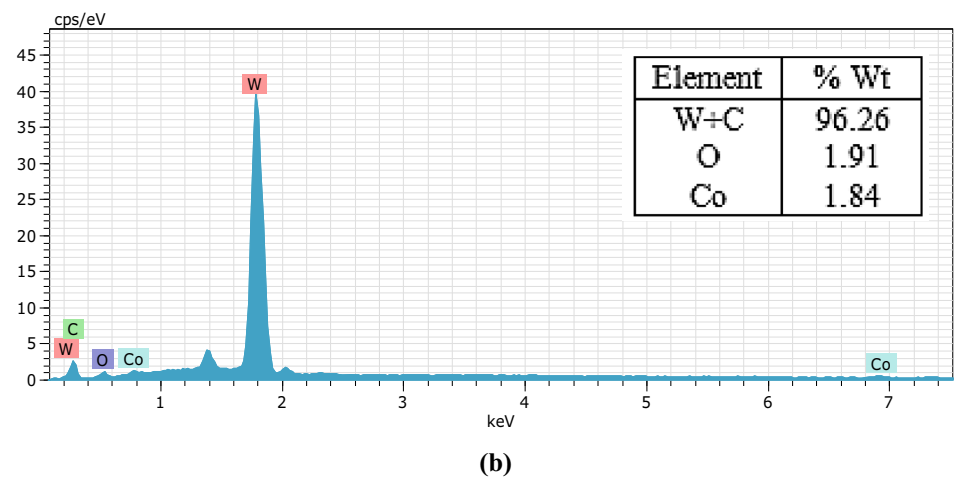
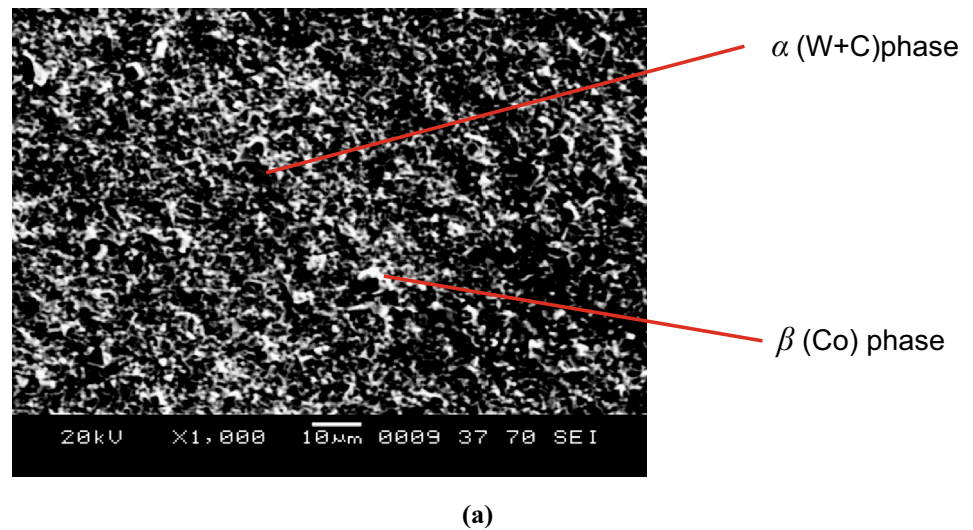
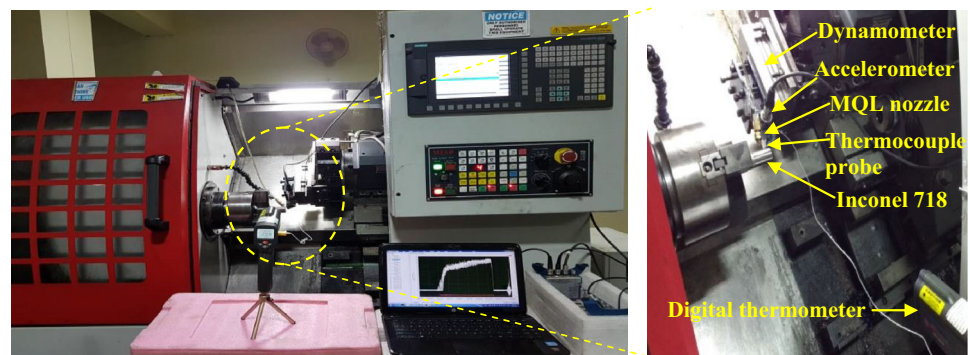


Fig. 5 Experimental setup (left) and measuring instrument in turning of Inconel 718 (right)



The additional axial points basically raise the number of levels to five where distance of the axial point from the design centre is $\alpha = 2^{k/4}$. CCD including axial points with the designed value α is called circumscribed central composite design placed on the coordinate axis of the factorial segment at a supplementary distance of $\alpha = 1.682$ from the centre. Due to rotatable design of central composite design, it is observed that, when $\alpha > 1$, the run for every

independent variable is at five levels and are denoted by $-1.682, -1, 0, +1, +1.682$ as shown in Fig. 6. Thus, a great deal of information is accumulated about the effects of the factors and their interactions.

Experimental design uses variation of three input parameters—cutting speed (v), feed rate (f) and depth of cut (d) whose five levels are coded. The coded and normal levels of the input variables are tabulated in Table 1. The outcome of design of experiment (DOE) shows 20

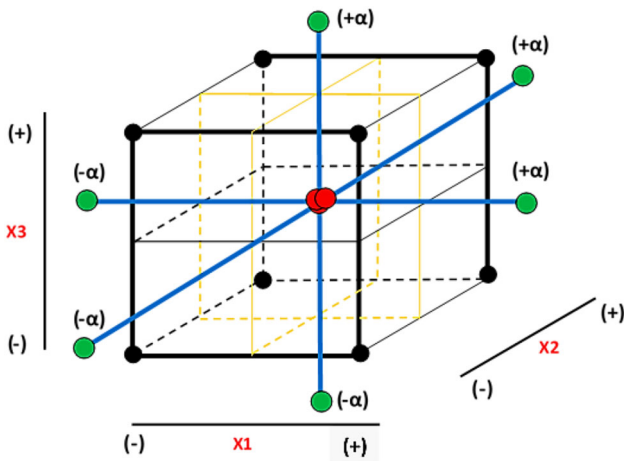


Fig. 6 Central composite design for factors

experiments along with six duplication of centre point according to the CCD, using RSM in MINITAB 17 software. The design matrix of input and measured values are presented in Table 2. The measured values of cutting force (F_c), tool vibration (A_s), cutting temperature (T), surface roughness (R_a), and tool flank wear (VB_{max}) for the four conditions used, i.e. DRY, DRY-CT, MQL and MQL-CT are listed in Table 2.

3 RSM modelling

Response surface method determines relationship among independent variables and dependent variables [38, 39]. In RSM, the second-order model is generally used due to its simplicity, flexibility and ability to estimate the correct response surface parameters. The values of output variables are measured experimentally from the machining process and input–output relationship is determined using RSM methodology in MINITAB 17 software. The empirical relationships (prediction models) establish correlation between output parameters (F_c , A_s , T , R_a and VB_{max}) and cutting parameters (v , f , d) in the turning of Inconel 718. By statistical analysis, the adequacy of developed models, for four machining conditions, was verified using analysis of variance (ANOVA) to determine the significant and non-significant parameters on the basis of p (probability) values, F values and correlation coefficient (R^2). These are

shown in Table 3a–d. The p value less than 0.05 specifies that model variables are significant and p values greater than 0.05 show the insignificant variables of model for confidence limit of 95% [38]. The larger values of F and smaller values of p ($p < 0.05$) show that models are significant. The R^2 nearer to unity indicates best correlation between predicted data of model and experimental data.

3.1 Refinement of developed model using backward elimination method

To remove insignificant effects from developed models, the backward regression elimination method is used to find a best fit model. In this method, a test for significance is performed on the variables. The largest p value of the variable is eliminated based on value specified in predefined level. The modified (refined) models are obtained with significant variables and then used for further regression analysis. The modified models suitable for estimating F_c , A_s , T , R_a and VB_{max} for all machining conditions on basis of fine R^2 and R^2 adj values are presented in Eqs. (1)–(20).

Refined models for dry turning with untreated inserts:

$$F_c = 783.8 - 4.822v + 604f + 146.9d \quad (R^2 = 92.35) (R^2 \text{ adj} = 90.92) \quad (1)$$

$$A_s = 2.14 - 0.0295v + 16.4f - 0.80d + 0.000270v^2 + 115.4f^2 + 4.86d^2 - 0.2492vf - 35.3fd \quad (R^2 = 94.43) (R^2 \text{ adj} = 90.38) \quad (2)$$

$$T = 681.9 + 1.139v + 1019f + 100.2d - 0.00574v^2 - 2296f^2 + 5.25vf + 0.95vd - 670fd \quad (R^2 = 98.64) (R^2 \text{ adj} = 97.64) \quad (3)$$

$$R_a = 6.466 - 0.04145v - 25.25f - 4.93d + 0.000211v^2 + 69.5f^2 + 2.520d^2 + 11.80fd \quad (R^2 = 93.08) (R^2 \text{ adj} = 89.05) \quad (4)$$

$$VB_{max} = 0.129 + 0.00973v + 5.40f + 0.1708d - 0.000046v^2 - 15.25f^2 \quad (R^2 = 90.34) (R^2 \text{ adj} = 86.84) \quad (5)$$

Refined models for dry turning with cryo-treated inserts:

Table 1 Level of cutting parameters for the turning of Inconel 718

Cutting parameters	Level 1	Level 2	Level 3	Level 4	Level 5
Coded values	- 1.682	- 1	0	1	1.682
Cutting speed, v (m/min)	9.5	30	60	90	110.45
Feed rate, f (mm/rev)	0.06	0.1	0.15	0.2	0.23
Depth of cut, d (mm)	0.32	0.5	0.75	1	1.17

Table 2 Design matrix and experimental result (DRY/DRY-CT/MQL/MQL-CT)

Run	v (m/min)	f (mm/rev)	d (mm)	Responses for—DRY/DRY-CT/MQL/MQL-CT				
				F_c (N)	A_s (g)	T (K)	R_a (μ m)	VB_{max} (mm)
1.	90	0.2	1	626/593/553/492	1.8/2.18/1.76/1.83	995/970/795/713	2.2/1.56/1.41/0.74	1.24/1.132/1.02/0.98
2.	9.5	0.15	0.75	881/854/805/753	4.71/4.56/3.53/4.09	810/710/610/520	2.89/2.22/2.13/1.19	0.84/0.79/0.64/0.55
3.	30	0.2	0.5	837/813/772/712	5.3/4.61/4.04/3.18	852/722/659/560	2.57/0.98/1.8/0.91	0.88/0.787/0.63/0.59
4.	60	0.06	0.75	622/590/562/491	2.1/2.01/1.87/1.52	890/732/710/610	1.68/0.87/0.91/0.65	0.9/0.803/0.67/0.63
5.	60	0.15	0.75	684/660/623/561	2.3/1.82/1.81/1.63	920/819/740/643	1.47/1.27/0.71/0.71	1.15/1.051/0.91/0.87
6.	60	0.15	1.17	737/695/625/596	4.12/3.82/3.65/3.11	940/910/788/657	2.49/1.67/1.73/0.9	1.21/1.1/0.99/0.93
7.	110.45	0.15	0.75	448/415/403/316	1.23/1.33/0.93/0.83	998/986/818/730	1.24/0.72/0.51/0.58	1.25/1.12/1.03/0.98
8.	30	0.2	1	853/823/788/724	4.56/4.13/3.62/3.47	850/750/668/570	2.85/1.87/2.11/0.96	0.98/0.966/0.82/0.71
9.	60	0.15	0.75	702/667/632/568	2.39/2.01/1.81/1.63	930/780/748/681	1.54/0.72/0.78/0.72	1.13/1.061/0.87/0.8
10.	60	0.15	0.75	687/655/605/556	2.21/1.82/1.69/1.29	928/770/752/632	1.65/0.86/0.93/0.73	1.17/1.093/0.94/0.89
11.	90	0.2	0.5	540/520/471/421	2.43/1.76/1.75/1.43	980/910/756/765	1.7/0.81/0.95/0.7	1.15/1.061/0.95/0.88
12.	90	0.1	1	576/540/499/442	2.98/1.61/1.73/1.21	985/950/786/700	1.32/0.46/0.58/0.7	1.18/1.09/0.93/0.87
13.	60	0.23	0.75	807/748/703/648	4.11/3.22/3.08/2.94	912/860/755/684	2.34/1.56/1.63/0.91	1.21/1.112/1.01/0.96
14.	60	0.15	0.75	717/657/615/556	2.18/2.54/1.91/1.22	925/780/752/726	1.69/1.48/0.94/0.7	1.19/1.101/0.97/0.95
15.	30	0.1	1	872/821/785/722	3.73/3.52/2.53/2.12	860/720/650/580	2.27/1.37/1.49/0.88	0.92/0.812/0.69/0.65
16.	30	0.1	0.5	865/815/776/716	3.22/3.2.73/2.42	840/680/638/525	2.67/1.42/1.91/0.87	0.9/0.797/0.68/0.61
17.	60	0.15	0.75	700/663/627/564	2.34/2.1/1.76/1.31	923/785/741/638	1.51/0.93/0.76/0.74	1.16/1.089/0.96/0.92
18.	60	0.15	0.32	586/646/606/545	2.21/2.54/1.89/1.41	880/680/693/560	1.48/0.87/0.75/0.68	1/0.894/0.77/0.75
19.	60	0.15	0.75	720/681/633/582	2.37/2.09/1.54/0.98	915/728/758/630	1.52/0.91/0.76/0.7	1.15/1.086/0.95/0.9
20.	90	0.1	0.5	437/420/374/321	1.33/1.43/0.92/0.81	925/880/748/640	1.32/0.81/0.58/0.6	1.16/1.051/0.92/0.88

Table 3 Summarized results of ANOVA for second-order polynomial prediction model

Source	Parameters	Regression model	ν	f	d	ν^2	f^2	d^2	νf	νd	fd	R^2	R^2 (adjusted)
(a) Models for dry turning with untreated inserts													
Cutting force (F_c)	F ratio	30.28	240.8	10.02	15.60	0.98	0.73	1.18	4.11	4.20	0.20	96.46	93.28
	p value	< 0.0001	< 0.0001	< 0.01	0.003	0.346*	0.412*	0.302*	0.070*	0.068*	0.665*		
Tool vibration (A_s)	F ratio	22.02	109.37	20.53	12.02	6.93	10.19	11.20	9.11	1.59	109.37	95.20	90.87
	p value	0.000	0.000	0.001	0.006	0.025	0.010	0.007	0.013	0.236*	0.005		
Cutting temperature (T)	F ratio	104.14	790.15	17.57	54.60	7.79	9.92	2.92	8.81	7.21	9.96	98.94	97.99
	p value	0.000	0.000	0.002	0.000	0.019	0.010	0.118*	0.014	0.023	0.010		
Surface roughness (R_a)	F ratio	22.19	119.09	17.02	8.80	18.92	16.49	13.42	2.76	1.74	6.32	95.23	90.94
	p value	0.000	0.000	0.002	0.014	0.001	0.002	0.004	0.128*	0.216*	0.031		
Tool flank wear (VB_{max})	F ratio	15.13	90.46	13.61	9.57	11.33	10.23	2.94	0.01	0.01	1.17	93.16	87.00
	p value	0.000	0.000	0.004	0.011	0.007	0.010	0.117*	0.944*	0.944*	0.305*		
(b) Models for dry turning with cryogenically treated inserts													
Cutting force (F_c)	F ratio	62.09	515.30	23.24	11.72	1.94	0.34	0.52	5.40	7.23	0.43	96.66	87.01
	p value	0.000	0.000	0.001	0.007	0.194*	0.573*	0.489*	0.042	0.023	0.528*		
Tool vibration (A_s)	F ratio	21.58	131.62	17.49	5.73	10.64	4.14	18.01	2.18	0.39	0.72	95.10	90.70
	p value	0.000	0.000	0.002	0.038	0.009	0.069*	0.002	0.170*	0.545*	0.415*		
Cutting temperature (T)	F ratio	13.09	85.17	5.42	17.33	6.98	0.62	0.57	0.04	0.33	0.04	92.18	85.14
	p value	0.000	0.000	0.042	0.002	0.025	0.451*	0.469*	0.841*	0.576*	0.841*		
Surface roughness (R_a)	F ratio	5.35	23.21	5.08	5.21	2.93	0.21	0.49	1.99	0.36	7.64	82.81	67.33
	p value	0.007	0.001	0.048	0.046	0.118	0.655*	0.499*	0.189*	0.564*	0.020		
Tool flank wear (VB_{max})	F ratio	18.22	91.66	23.61	15.09	15.90	15.67	7.11	0.56	0.47	2.56	94.25	89.08
	p value	0.000	0.000	0.001	0.003	0.003	0.003	0.024	0.470*	0.509*	0.141*		
(c) Models for turning with MQL using untreated inserts													
Cutting force (F_c)	F ratio	37.03	310.46	12.22	6.04	0.37	0.48	0.00	3.34	4.79	0.19	97.09	94.47
	p value	0.000	0.000	0.006	0.034	0.555*	0.504*	0.966*	0.098*	0.054*	0.674*		
Tool vibration (A_s)	F ratio	15.22	79.94	16.58	7.06	2.46	7.51	14.02	2.76	2.41	1.21	93.20	87.07
	p value	0.000	0.000	0.002	0.024	0.148*	0.021	0.004	0.128*	0.151*	0.297*		
Cutting temperature (T)	F ratio	33.86	245.72	7.62	24.63	17.70	5.7111	2.76	0.31	1.98	0.00	96.82	93.96
	p value	0.000	0.000	0.020	0.001	0.002	0.038	0.128*	0.592*	0.189*	0.961*		
Surface roughness (R_a)	F ratio	21.51	114.41	17.77	7.95	18.39	16.21	13.01	2.14	1.46	6.36	95.09	90.67
	p value	0.000	0.000	0.002	0.018	0.002	0.002	0.005	0.174*	0.255*	0.030		
Tool flank wear (VB_{max})	F ratio	12.78	68.91	17.24	9.59	7.80	7.40	2.72	0.07	0.63	2.52	92.00	84.80
	p value	0.000	0.000	0.002	0.011	0.019	0.022	0.130*	0.797*	0.446*	0.143*		

Table 3 (continued)

Source	Parameters	Regression model	v	f	d	v^2	f^2	d^2	vf	vd	fd	R^2	R^2 (adjusted)
(d) Models for turning with MQL using cryogenically treated inserts													
Cutting force (F_c)	F ratio	59.36	492.97	21.64	11.62	0.33	1.93	0.47	5.13	6.72	0.43	98.16	96.51
	p value	0.000	0.000	0.001	0.007	0.195*	0.579*	0.510*	0.047	0.027	0.527*		
Tool vibration (A_s)	F ratio	12.27	63.51	14.07	6.03	10.64	6.71	6.48	0.66	0.57	0.30	91.70	84.22
	p value	0.000	0.000	0.004	0.034	0.009	0.027	0.029	0.437*	0.468*	0.595*		
Cutting temperature (T)	F ratio	9.94	64.36	6.79	5.52	1.73	0.07	4.15	1.69	0.43	3.26	89.95	80.90
	p value	0.001	0.000	0.026	0.041	0.218*	0.790*	0.069*	0.223*	0.527*	0.101*		
Surface roughness (R_a)	F ratio	11.63	74.40	9.25	6.56	11.33	1.00	1.50	0.01	0.23	0.01	91.28	83.44
	p value	0.000	0.000	0.012	0.028	0.007	0.341*	0.248*	0.908*	0.645*	0.908*		
Tool flank wear (VB_{max})	F ratio	11.54	66.22	12.40	5.92	10.44	6.79	2.21	0.18	0.18	1.33	91.22	83.31
	p value	0.000	0.000	0.006	0.035	0.009	0.026	0.168*	0.679*	0.679*	0.275*		

*Insignificant term for confidence limit of 95%

$$F_c = 1040.3 - 8.85v - 155f - 92.2d + 12.75vf + 2.95vd \quad (R^2 = 97.12)(R^2 \text{ adj} = 96.77) \quad (6)$$

$$A_s = 6.458 - 0.0673v + 7.39f - 7.06d + 0.000282v^2 + 5.27d^2 \quad (R^2 = 91.46)(R^2 \text{ adj} = 88.41) \quad (7)$$

$$T = 496.7 - 0.15v + 490f + 170.9d + 0.02770v^2 \quad (R^2 = 91.01)(R^2 \text{ adj} = 88.62) \quad (8)$$

$$R_a = 3.057 - 0.01104v - 11.93f - 2.31d + 20.40fd \quad (R^2 = 73.18)(R^2 \text{ adj} = 66.03) \quad (9)$$

$$VB_{max} = -0.277 + 0.00979v + 6.28f + 0.906d - 0.000051v^2 - 17.69f^2 - 0.479d^2 \quad (R^2 = 92.19)(R^2 \text{ adj} = 88.58) \quad (10)$$

Refined models for turning with MQL using untreated inserts:

$$F_c = 759.4 - 4.637v + 562f + 76.8d \quad (R^2 = 94.34)(R^2 \text{ adj} = 93.34) \quad (11)$$

$$A_s = 6.28 - 0.02717v - 18.1f - 6.35d + 87.1f^2 + 4.86d^2 \quad (R^2 = 87.18)(R^2 \text{ adj} = 82.60) \quad (12)$$

$$T = 409.3 + 3.993v + 1138f + 75.4d - 0.01661v^2 - 3208f^2 \quad (R^2 = 95.22)(R^2 \text{ adj} = 93.51) \quad (13)$$

$$R_a = 5.694 - 0.04103v - 25.16f - 4.93d + 0.000209v^2 + 69.3f^2 + 2.494d^2 + 11.90fd \quad (R^2 = 93.32)(R^2 \text{ adj} = 89.43) \quad (14)$$

$$VB_{max} = -0.090 + 0.00896v + 5.27f + 0.1903d - 0.000041v^2 - 14.02f^2 \quad (R^2 = 87.25)(R^2 \text{ adj} = 82.70) \quad (15)$$

Refined models for turning with MQL using cryo-treated inserts:

$$F_c = 937.6 - 8.79v - 160f - 87.9d + 12.67vf + 2.90vd \quad (R^2 = 97.53)(R^2 \text{ adj} = 96.64) \quad (16)$$

$$A_s = 6.74 - 0.0713v - 21.7f - 4.92d + 0.000362v^2 + 101.5f^2 + 4.00d^2 \quad (R^2 = 90.43)(R^2 \text{ adj} = 86.01) \quad (17)$$

$$T = 386.9 + 2.285v + 416f + 69.4d \quad (R^2 = 79.13)(R^2 \text{ adj} = 75.21) \quad (18)$$

$$R_a = 0.8465 - 0.01125v + 1.007f + 0.1661d + 0.000055v^2 \quad (R^2 = 89.09)(R^2 \text{ adj} = 86.18) \quad (19)$$

$$\text{VB}_{\max} = -0.341 + 0.01061v + 5.36f + 0.1618d - 0.000052v^2 - 14.68f^2 \quad (R^2 = 87.79)(R^2 \text{ adj} = 83.43) \quad (20)$$

The ANOVA is used again to evaluate significance of modified regression models for p and F ratio values. The p value less than 0.05 and high F values of the modified models indicate that the models are extremely significant. The parameters v , f and d are found significant for all the modified models. Therefore, these models can produce better results compared to models with insignificant terms, when same ranges of cutting parameters are utilized in the modified model.

Using input data from Table 2 in Eqs. (1)–(20), the estimated response values are evaluated. The estimated values obtained by RSM modified models are compared with the measured responses. The comparison of estimation capability of RSM with experimental values based on R^2 values, R^2 adj values and percentage of mean absolute error (MAE) is carried out. The obtained percentages of mean absolute error (MAE) along with R^2 values and R^2 adj values are tabulated in Table 4 for the four machining conditions DRY, DRY-CT, MQL and MQL-CT, respectively, for individual responses. It is observed that for most of the responses MAE is less than 15%. Based on R^2 value and MAE, it is found that these models are acceptable for further analysis.

4 Pictorial representation of models

The performance of the modified models is enumerated with different responses such as F_c , A_s , T , R_a and VB_{\max} . Figures 7, 8, 9, 10 and 11 list the plots of these models as

against cutting parameters v , f and d for different machining conditions—DRY, DRY-CT, MQL and MQL-CT. While plotting, one cutting parameter is varied and the others are kept constant at mid value. The performance models are plotted for evaluating the performance in the turning of Inconel 718 under different machining conditions.

4.1 Effect of cutting parameters on cutting force

Figure 7a represents the variation in cutting force for four cutting conditions against cutting speed, keeping feed and depth of cut constant at mid value. Similarly, Fig. 7b, c are plotted for variation of force with feed and depth of cut, respectively. In all the conditions, cutting speed is more significant parameter for the cutting force followed by feed rate. However, less significant variation is observed with respect to the depth of cut. These main effect plots clearly show that minimum F_c occurs at a higher v , lower f and d . However, it increases with increase in the f and d in all machining conditions. In DRY-CT condition, the cutting force required is slightly less than in DRY. Further, small reduction in cutting forces is observed for MQL compared to the DRY-CT condition due to the heat removal from the tool-chip edge and the lubrication between the cutting edge and the work piece. It is observed that amongst four conditions MQL-CT condition requires minimum cutting force.

4.2 Effect of cutting parameters on tool vibration

The vibration (acceleration) of the tool was measured with respect to the varying cutting parameters and results are shown in Fig. 8. There is a prominent decrease in tool vibrations with increasing v . However, for increasing f and d up to a certain threshold value (0.15 mm/rev and 0.75 mm, respectively) minimum vibrations are observed. Beyond this threshold value the tool vibrations increase rapidly in all conditions. In DRY condition more tool vibrations are observed. While, the decreasing trends of

Table 4 Estimated accuracies of modified models

Response parameters	DRY			DRY CT			MQL			MQL CT		
	R^2 (%)	R^2 adj (%)	MAE (%)	R^2 (%)	R^2 adj (%)	MAE (%)	R^2 (%)	R^2 adj (%)	MAE (%)	R^2 (%)	R^2 adj (%)	MAE (%)
F_c	92.35	90.92	3.81	97.12	96.77	2.27	94.34	93.34	3.85	93.53	96.64	2.74
A_s	94.43	90.38	7.20	91.46	88.41	10.42	87.18	82.60	11.87	90.43	86.01	12.29
T	98.64	97.64	0.50	91.01	88.62	3.11	95.22	93.51	1.49	79.13	75.21	3.41
R_a	93.08	89.05	2.85	73.18	66.03	18.24	93.22	89.43	9.73	89.09	86.18	12.94
VB_{\max}	90.34	86.84	3.21	92.19	88.58	3.15	87.25	82.70	4.90	87.79	83.43	21.16

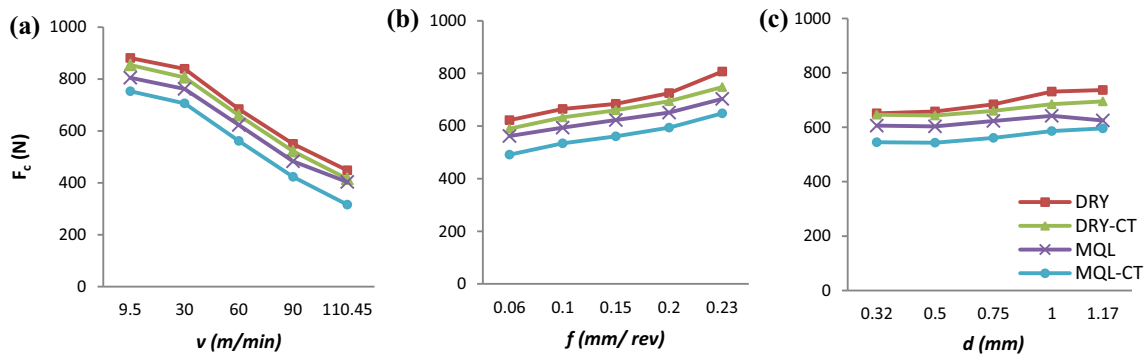


Fig. 7 Effect of cutting parameters on cutting force (F_c)

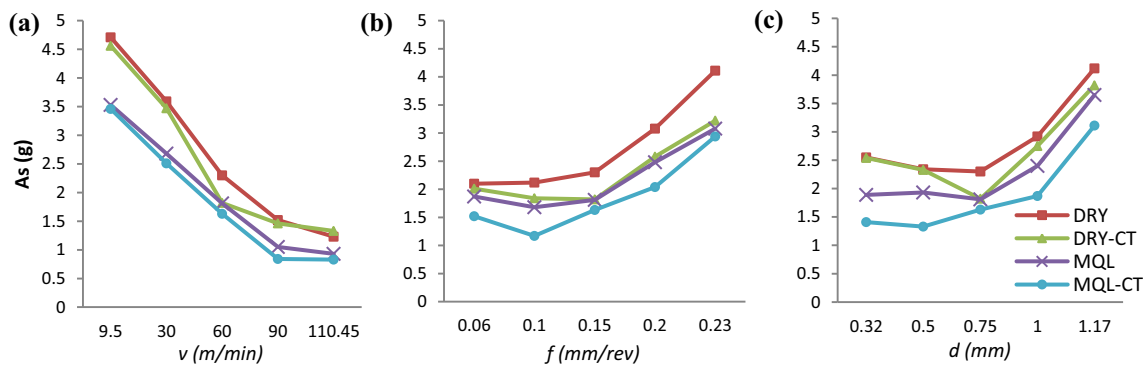


Fig. 8 Effect of cutting parameters on tool vibrations (A_s)

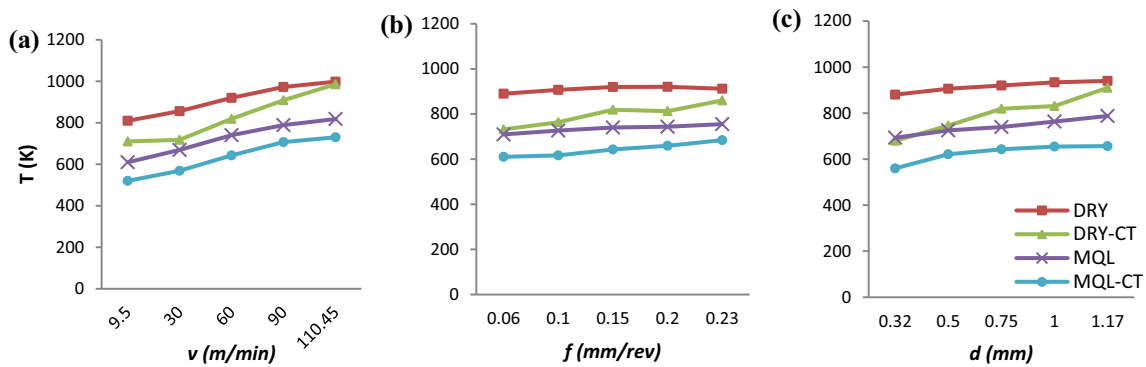


Fig. 9 Effect of cutting parameters on temperature (T)

tool vibrations are shown in DRY-CT, MQL and MQL-CT conditions.

4.3 Effect of input parameters on cutting temperature

Increase of cutting speed indicates a substantial increase in the cutting temperature than the rise which occurs with increase in feed and depth of cut (Fig. 9a–c). In MQL-CT condition, cutting temperature reduces because of lubricity through the deformation zone mainly at tool-chip edge than

DRY-CT and MQL. DRY condition shows highest temperature and MQL-CT shows lowest temperature.

4.4 Effect of cutting parameters on surface roughness

Figure 10a shows that there is a pronounced improvement in the surface roughness value with increasing cutting speed. However, for feed and depth of cut, the improvement in the surface roughness is found only up to a certain threshold value as visible in Fig. 10b, c, respectively.

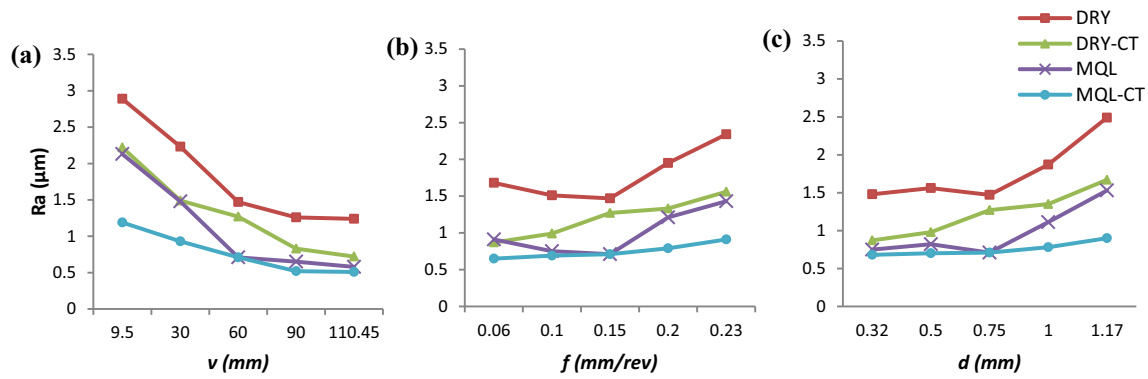


Fig. 10 Effect of cutting parameters on surface roughness (R_a)

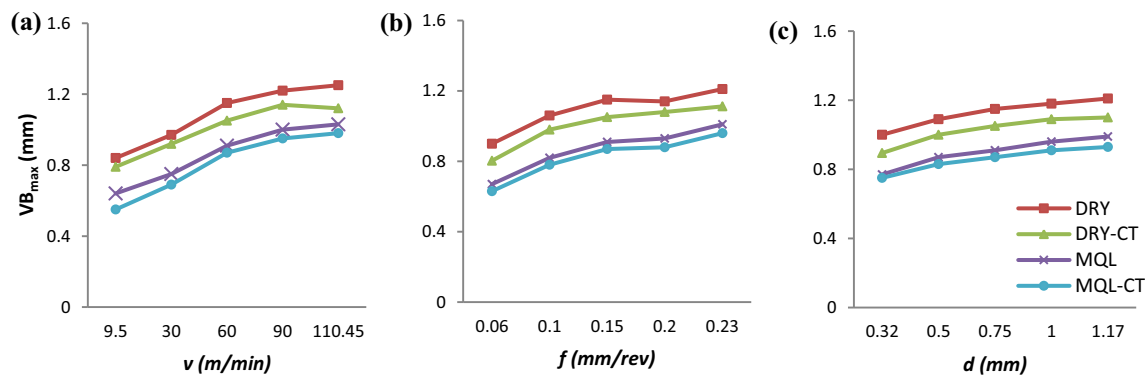


Fig. 11 Effect of cutting parameters on tool wear (VB_{\max})

Beyond this value, the surface finish degrades. This behaviour is observed prominently for the DRY and MQL condition. It is seen that, MQL and MQL-CT conditions achieve the best result (0.5–0.7 R_a for high v , low f and d) compared to the other conditions.

4.5 Effect of cutting parameters on tool wear

The variations of tool wear against v , f and d are shown in Fig. 11. The tool wear is similar for almost all the machining conditions. The effect of change of cutting speed influences the tool wear to a greater extent than f and d as observed in the Fig. 11a. There is variation in the tool wear values for the varying f and d for the different machining conditions as found in the Fig. 11b, c. The wear of the tool is the most severe in the DRY condition because of intense heat generation and material removal. The rate of material removal from tool flank face progressively reduces for different machining conditions, beginning from maximum for the DRY condition and minimum for the MQL-CT condition.

4.6 Effect of cutting conditions on machinability

It is observed that amongst all the machining conditions shown in Fig. 7a, the value of cutting force (F_c) is highest for the DRY condition at low cutting speed (v). It is known that Inconel 718 is hard to cut material. At high v , the reducing trend of the F_c is attributed to the low coefficient of thermal conductivity of Inconel 718, on account of which, the heat is built up in the work piece which causes it to soften [21, 40]. The temperature rise with cutting speed is clearly seen in Fig. 9a and this temperature rise is responsible for softening of work piece and reduction in cutting force.

It is seen from Fig. 7b that F_c increases as the feed (f) increases for all the machining conditions. The reason for this trend is that at high f , large amount of material comes in contact with tool in less time. Thus, high f is responsible for generating high friction.

According to Fig. 7c, depth of cut (d) shows less significant effect on F_c compared to effect of v and f amongst all machining conditions. Increasing d leads to increase in volume of material removal which only lengthens the contact but force/unit length remain stable [6]. As reported in literature [13, 41], more increase of d result in breaking

and chipping of cutting tool which drastically increases R_a and VB_{\max} . It was observed that sometimes breakage and chipping of tool affect continuity of machining process.

As the v increases, the F_c is reduced (Fig. 7a). This affects the deflection of tool also. More F_c means more deflection and vice versa. Since, the tool vibration (A_s) is the effect of interaction between machining process and the machine tool, lesser tool force results into lesser A_s and, therefore, increase in speed (v) shows reduction in vibrations (Fig. 8a). As the tool vibrations are reduced with speed, a better surface finish is obtained with increase in speed (Fig. 10a). Similarly, the vibration change with feed and depth of cut (Fig. 8b, c) affects the surface roughness, R_a (Fig. 10b, c).

In case of tool wear (Fig. 11), a direct correlation is seen with temperature (Fig. 9). With increase in all the cutting parameters, the temperature is showing an increasing trend and therefor, the tool wear also shows the same trend.

The highest temperature is observed in DRY condition which results in higher VB_{\max} , whereas slightly less VB_{\max} in DRY-CT condition. Further using MQL, the T and VB_{\max} values are reduced. Because of cooling and lubrication at cutting edge, the reduction of T is demonstrated in Fig. 9. Thus, MQL-CT condition results in least amount of wear due to least cutting temperature.

The cryogenic treatment results in microstructure change which are responsible for the increased wear resistance of the cutting tool and helps to retain its sharpness even at high temperature. Improvement in hardness enhances wear resistance of the tool and higher thermal conductivity helps for rapid heat conduction in tool, reducing temperature. Using cryogenically treated tools, the cutting force, vibration and cutting temperature are observed to be less compared to untreated tool in DRY turning of Inconel 718. The combined effect of all these responses is observed on the reduction in the surface roughness and tool wear values.

Further using MQL, the cutting temperature and tool wear values are reduced. Because, MQL achieves dual motives of heat removal from the tool-chip edge and the lubrication between the cutting edge and the work piece. The air stream continuously cools down the cutting zone while the micro-droplets of lubricant ensure proper lubrication by providing smooth layer at tool-chip interface. Moreover, MQL reduces the environmental impact by significantly decreasing cutting fluid usage and eliminating the necessity of coolant treatment, disposal, etc.

The combined effect of MQL with cryogenically treated tool in turning of Inconel 718 results in minimum cutting force, vibration, cutting temperature and surface roughness. Besides, MQL-CT condition contributes to good tool life which offers better productivity among other cutting

conditions. Overall MQL-CT gives the best possible reduction in all response parameters.

The goal in machining is achievement of good quality machined products at low cost with negligible damage to the environment and the human health. Looking into the economic aspect of machining, it is imperative that it can be improved by optimizing the machining parameters. Therefore, it was deemed to be necessary to determine an optimum value of the input cutting parameters for the desired output parameters.

5 Optimization of parameters using RSM

For turning of Inconel 718 combined optimization of the cutting parameters— v , f and d with the aim of minimization of F_c , A_s , T , R_a and VB_{\max} for DRY, DRY-CT, MQL and MQL-CT conditions are performed. RSM optimization analysis is performed for all modified models of four machining conditions using default values in MINITAB 17 software.

Multi-objective optimization is carried out in MINITAB 17 software which displays the global desirability solution, by default. Various points are picked up for the search of optimal values of variables in starting of optimization algorithm procedures. Local and global solutions are two solution types for the search. Out of all local solutions, only one best solution is the global solution and it is categorized as the best relation between independent variables for attaining the best possible response. RSM optimization method has various benefits over conventional experimental or optimization methods, where at a time, only one variable can be used. Also, RSM offers economically better method as a lesser number of experiments are required to get effects of main parameters and interaction among parameters. Therefore, in present work, response surface-based desirability approach [38, 42, 43] has been used for optimizing the response parameters in turning of Inconel 718. All the values of the response function are transformed into a dimensionless desirability value (d) that varies over the range $0 \leq d \leq 1$. The value, $d = 0$, suggests that the response is completely unacceptable, and $d = 1$ suggests that the response is acceptable and desirable. The individual desirability values (d_i) are combined with geometric mean. Thus, the overall desirability objective function is obtained by Eq. (21).

$$D = \left(\prod_{i=1}^n d_i^{r_i} \right)^{\frac{1}{\sum r_i}} \quad (21)$$

where D is the overall desirability objective function. The value of r is the response importance relative to the other response parameters of the process. The high value of

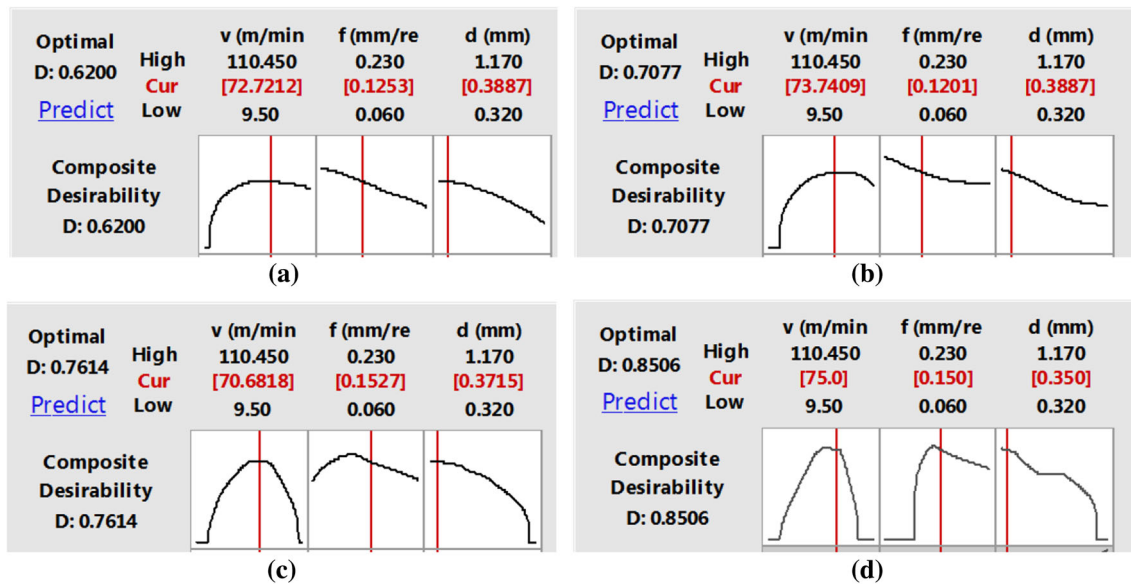


Fig. 12 RSM optimization: a DRY; b DRY-CT; c MQL; d MQL-CT

overall desirability D indicates the more desirable and the best function of the system. This indicates that the optimum value is reached. The optimum values of factors are determined from value of individual desired function that enhances the overall desirability value. Figure 12 shows the optimum cutting parameters with overall desirability values of 0.62, 0.70, 0.76 and 0.85 for DRY, DRY-CT, MQL and MQL-CT conditions, respectively. So, these responses are accepted. The values of inputs parameters are chosen for further experimentation.

5.1 Validation of results

Three confirmation experiments were performed for each condition using optimum values of cutting parameters obtained by RSM methodology for all response parameters together. The results obtained and percentage error are presented in Table 5. Thus, it is seen that the estimated values by modified Eqs. (1)–(20) correlate well with the experimental values.

It is observed from Table 5 that the errors for T , R_a and VB_{max} are less than 10% whereas overall error is higher in

case of vibration and this is natural because vibration contains the effect of machining process and the machine tool. It is also seen that MQL-CT condition gives best values of response parameters.

Economics of machining can be enhanced using optimum cutting parameters with proper machining conditions shown in Fig. 12 and Table 5. The main objective of this experimentation is to identify best machining conditions for minimizing surface finish, tool wear with maximum material removal rate. Therefore, to know the productivity for the used machining condition, it is essential to determine the material removal rate of workpiece (MRR) [44]. The optimum cutting parameters obtained from Fig. 12 are selected for getting the maximum MRR. These parameters would be useful to study MRR which can be calculated as, $MRR (mm^3/min) = 1000 \times v \times f \times d$.

5.2 Spider plot for confirmation experiment using optimum parameters

A spider plot is an excellent tool for having an overview by organizing complex information in a simple manner. It is

Table 5 Comparisons and confirmation of optimization result

Machining conditions	F_c (N)			A_s (g)			T (K)			R_a (μ m)			VB_{max} (mm)		
	Expt.	RSM	Error %	Expt.	RSM	Error %	Expt.	RSM	Error %	Expt.	RSM	Error %	Expt.	RSM	Error %
DRY	578	565.85	2.1	2.01	1.71	14.92	920	906.93	1.42	1.5	1.53	2	0.98	1.0	4.04
DRY-CT	557	530.43	4.77	1.98	1.96	1.01	810	761.9	5.93	0.90	0.86	4.45	0.90	0.94	4.44
MQL	498	446.07	10.42	1.8	1.94	7.21	771	735.52	4.60	0.73	0.80	8.75	0.81	0.88	8.64
MQL-CT	435	442.05	1.62	1.35	1.23	8.88	630	644.95	2.37	0.48	0.52	8.33	0.55	0.59	7.27

graphical method of presenting multivariate facts in the form of 2D chart. Distinguishing feature of spider plot is use of separate scales for every parameter on the same plot [15, 45]. It can help in obtaining specified response for the stipulated condition. Therefore, this plot is selected for showing data of confirmation experiments with optimum conditions, under the four conditions used for machining of Inconel 718.

To get the spider diagram, a polygon is drawn with number of vertices equal to the number of parameters. It is required to show the effect of three cutting parameters on six responses. Therefore, a polygon having nine vertices is drawn. Each of the nine parameters (three input + six responses) are represented by lines starting from centre and joining each vertex of the polygon. The minimum value of each parameter is kept as zero and is at the centre; whereas, maximum values are at the vertices of polygon. The associations among inputs and responses are presented using data of Table 6. Parameter values are marked on the line joining centre to vertex by considering proportionate scale and lines are drawn to connect the points falling under same cutting conditions. Thus, the spider plot is generated as shown in Fig. 13.

As seen from the spider plot, the curve obtained for MQL-CT represents the best machining condition for the machining of Inconel 718, which is at moderate cutting speed (75 m/min), medium feed (0.15 mm/rev) and low depth of cut (0.35 mm) leading to low value of cutting force, tool vibration, cutting temperature, tool wear and surface roughness. Besides, MQL-CT condition contributes to more material removal rate which offers better productivity among other optimum conditions.

Thus, MQL-CT condition resulted in 25, 22 and 13% lowering of F_c , 33, 32 and 25% decrease of A_s , 32, 22 and 18% lesser T , 68, 47 and 34% drop in R_a of the work piece, 44, 39 and 32% better tool life and 16, 14 and 0.4% improvement in MRR compared to that of DRY, DRY-CT and MQL conditions, respectively. Thus, MQL-CT condition results in the best machining of Inconel 718 with desired surface quality needed for high precision parts. Figure 14a–d demonstrates the surface topography of machined surface. The enhancement in surface texture is

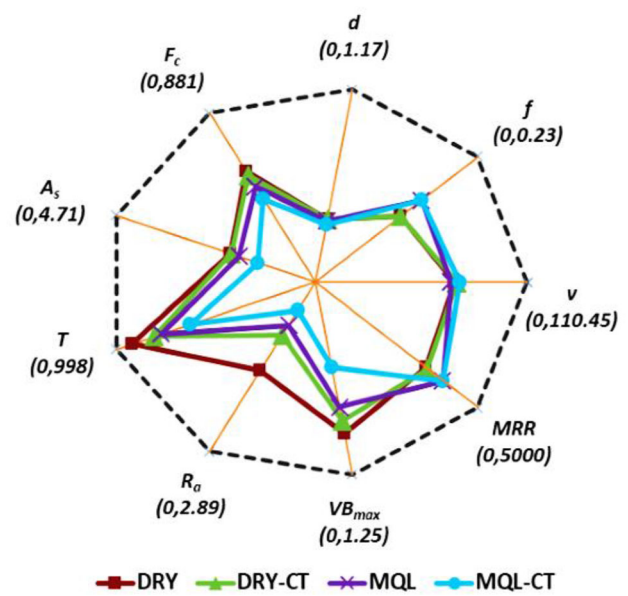


Fig. 13 Spider plot for optimum machining conditions

noticeable from 3D optical profilometer which reveals a better topography of workpiece surface machined with MQL-CT condition as seen in Fig. 14d.

The flank wear at nose region is measured at a different cutting lengths using optimum parameters and the performance of tool is presented in Fig. 15. The corresponding tool wear at the end of each machining condition is shown in Fig. 16a–d for four machining conditions. Spider plot clearly shows higher and lower values of R_a and VB_{max} which is evidenced in Figs. 14, 15 and 16. The high values of R_a , VB and low MRR are observed in DRY machining. In DRY-CT condition, slight reduction in R_a , VB_{max} and improvement in MRR is observed due to cryo treatment. The hardness of untreated insert was found to be 1474 VHN and that of cryo-treated insert was found to be 1576 VHN. Thus, the erosion of the material from the tool flank is reduced which also helped in slight improvement of surface finish. By employing MQL, there is reduction of all responses except MRR. Because of good lubricity between tool and chip, there is significant improvement in surface roughness. MQL results in immediate lowering of the tool-

Table 6 Optimum parameters and limiting values for spider plot

Conditions	v (m/min)	f (mm/rev)	d (mm)	F_c (N)	A_s (g)	T (K)	R_a (μ m)	VB_{max} (mm)	MRR (mm^3/min)
DRY	72.72	0.12	0.38	578	2.01	920	1.5	0.98	3403
DRY-CT	73.74	0.12	0.38	557	1.98	810	0.9	0.9	3451
MQL	70.68	0.15	0.37	498	1.8	771	0.73	0.81	3922
MQL-CT	75	0.15	0.35	435	1.35	630	0.48	0.55	3938
Min	0	0	0	0	0	0	0	0	0
Max	110.45	0.23	1.17	881	4.71	998	2.89	1.25	5000

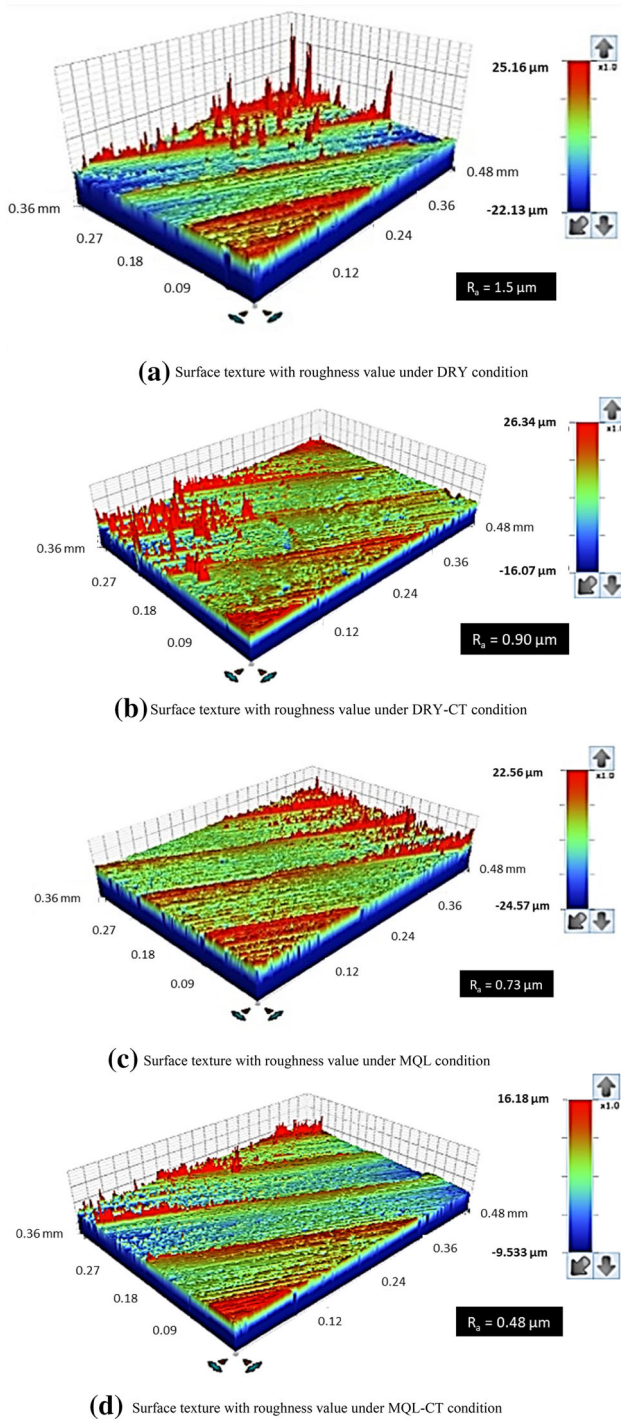


Fig. 14 Surface roughness at optimum parameters

chip interface temperature value because of which the tendency of the flank wear at nose region is reduced. The low values of F_c , A_s , and T ultimately improve the R_a value compared to other conditions. The reduction in T also implies reduction in the VB_{\max} evidenced in Figs. 15 and 16. The least amount of wear is achieved on tool which deforms less with MQL-CT condition as seen in Fig. 16d.

It is because, MQL spray provides the penetration of the lubricant within the tool-chip interface and helps for heat dissipation; cryo treatment improves wear resistance and provides harder tool edges. As a result, the performance of tool is enhanced which reflects on the quality of machined surface.

6 Conclusion

In the present study, turning of Inconel 718 was performed under four machining conditions. Models were developed for five response parameters, i.e. cutting force, vibration, temperature, surface roughness and tool wear. Analysis of variance (ANOVA) was performed on each model and the models were updated by removing insignificant terms. Later on, desirability approach was used to perform simultaneous optimization of all the responses. Predictions of the combined model were confirmed by confirmation experiments. On the basis of this experimental study, following conclusions are drawn.

- Cryogenic treatment changed the microstructure of tool which improved hardness of tool by 7% along with improvement in electrical conductivity by 14.83%. Improvement in hardness enhances wear resistance of the tool and higher thermal conductivity helps for rapid heat conduction in tool reducing temperature and tool wear.
- Analysis of variance is used to evaluate significant parameters of modified regression models for p and F ratio values. The p value less than 0.05 and high F values of the modified models indicate that the models are extremely significant. Moreover, it is observed that cutting speed is the most significant parameter for all the responses, followed by feed and depth of cut in most of the machining conditions.
- The ANOVA of the prediction models developed by RSM for five response parameters (cutting force, vibration, temperature, surface roughness and tool wear) showed good association between measured and estimated values. This was indicated by the R^2 (correlation coefficient) values. The modified regression models using RSM are having R^2 values in range of 73.18–99.72%. The R^2 closer to unity indicates best correlation between predicted data of model and experimental data. Additionally, the adequacy of models was examined by percentage of mean absolute error (MAE). It was observed that the MAE was obtained as less than 15% in most of the machining conditions. Based on prediction accuracy, it is concluded that the modified models accurately predict the responses.

Fig. 15 Performance of tools at optimum parameters in DRY, DRY-CT, MQL and MQL-CT conditions

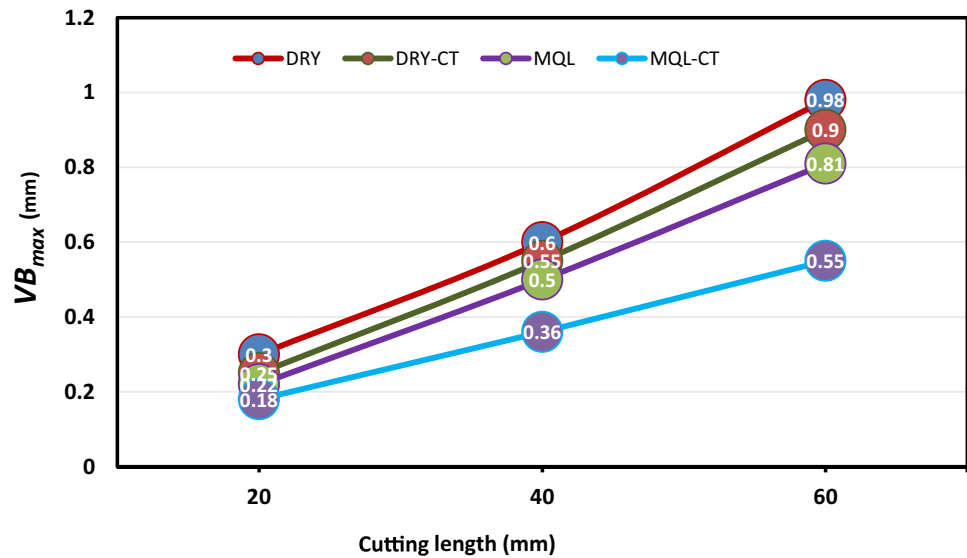
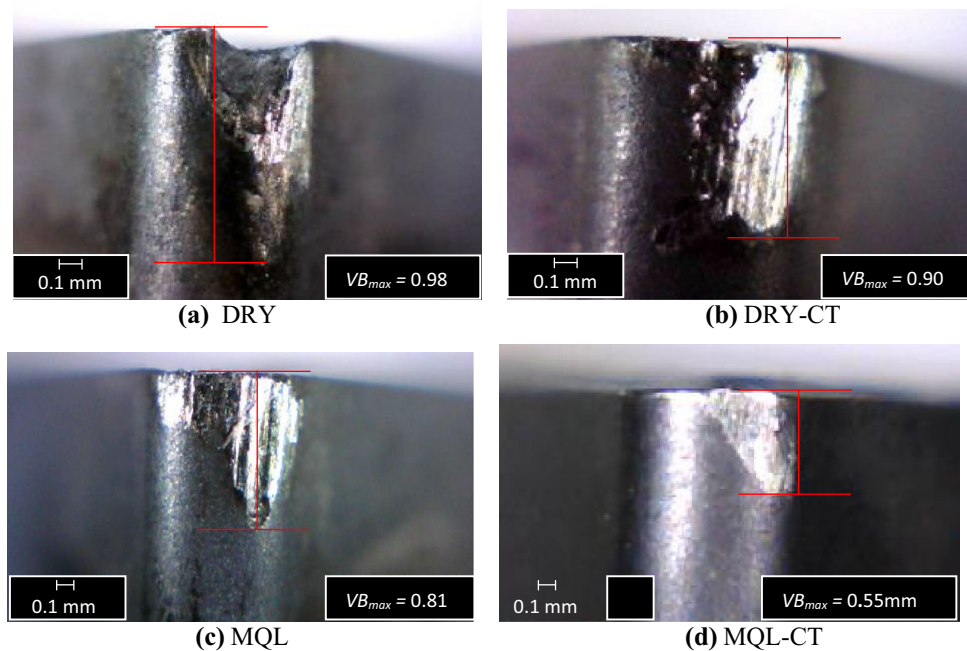


Fig. 16 Variations of flank wear at nose region using optimum cutting parameters



- Comparing machining with untreated insert in DRY and MQL conditions, the use of MQL resulted in 14% reduction in force, 10% decrease of vibration, 16% lowering of temperature, 51% enhancement in surface finish, 17% improvement in tool life and 15% improvement in material removal rate which are helpful to increase the productivity.
- The machining performance can be further improved using MQL with cryo-treated inserts. MQL prominently helps in improving the performance of tool due to better heat dissipation from cutting region and cryo treatment improved wear resistance. Comparing untreated and cryo-treated insert; the use of cryo-

- treated insert resulted in 4% reduction in force, 1.50% decrease of vibration, 12% lowering of temperature, 40% enhancement in surface finish, 8% improvement in tool life and 1.50% improvement in material removal rate. Hence, the characteristics of cryo-treated inserts reflect on the quality of machined surface and tool life.
- Spider diagram was used to represent the best machining condition in turning of Inconel 718. The optimum condition is found for MQL-CT condition which is at moderate cutting speed (75 m/min), medium feed (0.15 mm/rev) and low depth of cut (0.32 mm). It can be further concluded that MQL-CT resulted in 25, 22 and 13% reduction in cutting force, 33, 32 and 25%

decrease of vibration, 32, 22 and 18% lowering of temperature than machining with DRY, DRY-CT and MQL conditions, respectively. Similarly, the use of MQL-CT also resulted in 68, 47 and 34% enhancements in surface finish; 44, 39 and 32% improvements in tool life and 16, 14 and 0.4% improvements in material removal rate, respectively. Thus, MQL-CT is identified as the best method for improving the overall productivity of the process.

- Hence, the use of cryogenically treated inserts with Minimum Quantity Lubrication is recommended for the turning of Inconel 718.

Acknowledgements This research work was financially supported by Technical Education Quality Improvement Program-II (TEQIP-II) Visvesvaraya National Institute of Technology, Nagpur, India. The authors sincerely thank to Mr. N Sahu and Mr. Parikshit Dumbhare for their assistance in the experimental work and also thankful to Mr. Purushottam Barve for his valuable support in treatment of tools.

References

- Pusavec F, Deshpande A, Yang S, M'Saoubi R, Kopac J, Dillon OW Jr, Jawahir IS (2014) Sustainable machining of high temperature Nickel alloy—Inconel 718: part 1—predictive performance models. *J Clean Prod* 81:255–269. <https://doi.org/10.1016/j.jclepro.2014.06.040>
- Arunachalam R, Mannan MA (2000) Machinability of nickel-based high temperature alloys. *Mach Sci Technol* 4(1):127–168
- Ezugwu EO (2005) Key improvements in the machining of difficult-to-cut aerospace superalloys. *Int J Mach Tools Manuf* 45(12):1353–1367
- Pervaiz S, Rashid A, Deiab I, Nicolescu M (2014) Influence of tool materials on machinability of titanium-and nickel-based alloys: a review. *Mater Manuf Process* 29(3):219–252
- Pawade RS, Joshi SS, Brahmankar PK (2008) Effect of machining parameters and cutting edge geometry on surface integrity of high-speed turned Inconel 718. *Int J Mach Tools Manuf* 48(1):15–28
- Thakur DG, Ramamoorthy B, Vijayaraghavan L (2012) Effect of cutting parameters on the degree of work hardening and tool life during high-speed machining of Inconel 718. *Int J Adv Manuf Technol* 59(5–8):483–489
- Wang ZY, Rajurkar KP (2000) Cryogenic machining of hard-to-cut materials. *Wear* 239(2):168–175
- Lalwani DI, Mehta NK, Jain PK (2008) Experimental investigations of cutting parameters influence on cutting forces and surface roughness in finish hard turning of MDN250 steel. *J Mater Process Technol* 206(1):167–179
- Blau PJ (2008) *Friction science and technology: from concepts to applications*. CRC Press, Boca Raton
- Benardos PG, Vosniakos GC (2003) Predicting surface roughness in machining: a review. *Int J Mach Tools Manuf* 43(8):833–844. [https://doi.org/10.1016/S0890-6955\(03\)00059-2](https://doi.org/10.1016/S0890-6955(03)00059-2)
- Tazehkandi AH, Shabgard M, Pilehvarian F (2015) Application of liquid nitrogen and spray mode of biodegradable vegetable cutting fluid with compressed air in order to reduce cutting fluid consumption in turning Inconel 740. *J Clean Prod* 108:90–103
- Kuram E, Ozcelik B, Demirbas E (2013) Environmentally friendly machining: vegetable based cutting fluids. In: Davim PJ (ed) *Green manufacturing processes and systems*. Springer, Berlin, pp 23–47
- Davoodi B, Tazehkandi AH (2014) Cutting forces and surface roughness in wet machining of Inconel alloy 738 with coated carbide tool. *Proc Inst Mech Eng Part B J Eng Manuf* 230(2):215–226 0954405414542990
- Debnath S, Reddy MM, Yi QS (2014) Environmental friendly cutting fluids and cooling techniques in machining: a review. *J Clean Prod* 83:33–47
- Pusavec F, Deshpande A, Yang S, M'Saoubi R, Kopac J, Dillon OW, Jawahir I (2015) Sustainable machining of high temperature Nickel alloy—Inconel 718: part 2—chip breakability and optimization. *J Clean Prod* 87:941–952
- Kaynak Y (2014) Evaluation of machining performance in cryogenic machining of Inconel 718 and comparison with dry and MQL machining. *Int J Adv Manuf Technol* 72(5):919–933. <https://doi.org/10.1007/s00170-014-5683-0>
- Gallagher AH, Agosti CD, Roth JT (2005) Effect of cryogenic treatments on tungsten carbide tool life: microstructural analysis. *Trans North Am Manuf Res Inst SME* 33:153–160
- Gill SS, Singh J, Singh H, Singh R (2012) Metallurgical and mechanical characteristics of cryogenically treated tungsten carbide (WC–Co). *Int J Adv Manuf Technol* 58(1–4):119–131
- Gill SS, Singh J, Singh H, Singh R (2011) Investigation on wear behaviour of cryogenically treated TiAlN coated tungsten carbide inserts in turning. *Int J Mach Tools Manuf* 51(1):25–33
- Gill SS, Singh R, Singh H, Singh J (2009) Wear behaviour of cryogenically treated tungsten carbide inserts under dry and wet turning conditions. *Int J Mach Tools Manuf* 49(3):256–260
- Deshpande Y, Andhare A, Sahu NK (2017) Estimation of surface roughness using cutting parameters, force, sound, and vibration in turning of Inconel 718. *J Braz Soc Mech Sci Eng* 39(12):5087–5096. <https://doi.org/10.1007/s40430-017-0819-4>
- Feyzi T, Safavi SM (2013) Improving machinability of Inconel 718 with a new hybrid machining technique. *Int J Adv Manuf Technol* 66(5–8):1025–1030
- Pawade RS, Joshi SS (2011) Multi-objective optimization of surface roughness and cutting forces in high-speed turning of Inconel 718 using Taguchi grey relational analysis (TGRA). *Int J Adv Manuf Technol* 56(1–4):47–62
- Homami RM, Tehrani AF, Mirzadeh H, Movahedi B, Azimifar F (2014) Optimization of turning process using artificial intelligence technology. *Int J Adv Manuf Technol* 70(5–8):1205–1217
- Tamang SK, Chandrasekaran M (2017) Integrated optimization methodology for intelligent machining of inconel 825 and its shop-floor application. *J Braz Soc Mech Sci Eng* 39(3):865–877
- Kumar KK, Choudhury SK (2008) Investigation of tool wear and cutting force in cryogenic machining using design of experiments. *J Mater Process Technol* 203(1):95–101
- Zurecki Z, Frey JH, Ghosh R (2003) Finish-turning of hardened powder-metallurgy steel using cryogenic cooling. *Adv Powder Metall Part Mater* 7:7–185
- Reddy TS, Ajaykumar B, Reddy MV, Venkataram R (2007) Improvement of tool life of cryogenically treated P-30 tools. In: *Proceedings of international conference on advanced materials and composites (ICAMC-2007) at the national institute for interdisciplinary science and technology, CSIR, Trivandrum, India*, pp 457–460
- Reddy TVS, Sornakumar T, Reddy MV, Venkatram R, Senthilkumar A (2009) Turning studies of deep cryogenic treated p-40 tungsten carbide cutting tool inserts—technical communication. *Mach Sci Technol* 13(2):269–281
- SreeramaReddy TV, Sornakumar T, VenkataramaReddy M, Venkatram R (2009) Machinability of C45 steel with deep

- cryogenic treated tungsten carbide cutting tool inserts. *Int J Refract Metal Hard Mater* 27(1):181–185
31. Deshpande YV, Andhare AB, Padole PM (2017) How cryogenic techniques help in machining of nickel alloys? A review. *Publ Mach Sci Technol Int J* (Taylor & Francis group)
32. Durand-Charre M (1998) *The microstructure of superalloys*. CRC Press, Boca Raton
33. WIDIA (2015) Turning catalogue. <https://www.widia.com>. Accessed 10 Aug 2016
34. Seah KHW, Rahman M, Yong KH (2003) Performance evaluation of cryogenically treated tungsten carbide cutting tool inserts. *Proc Inst Mech Eng Part B J Eng Manuf* 217(1):29–43
35. Stewart HA (2004) Cryogenic treatment of tungsten carbide reduces tool wear when machining medium density fiberboard. *For Prod J* 54(2):53
36. Yong AYL, Seah KHW, Rahman M (2007) Performance of cryogenically treated tungsten carbide tools in milling operations. *Int J Adv Manuf Technol* 32(7–8):638–643
37. Kenda J, Pusavec F, Kopac J (2011) Analysis of residual stresses in sustainable cryogenic machining of nickel based alloy—Inconel 718. *J Manuf Sci Eng* 133(4):041009
38. Myers RH, Montgomery DC, Anderson-Cook CM (2016) *Response surface methodology: process and product optimization using designed experiments*. Wiley, Hoboken
39. Noordin MY, Venkatesh VC, Sharif S, Elting S, Abdullah A (2004) Application of response surface methodology in describing the performance of coated carbide tools when turning AISI 1045 steel. *J Mater Process Technol* 145(1):46–58
40. Devillez A, Le Coz G, Dominiak S, Dudzinski D (2011) Dry machining of Inconel 718, workpiece surface integrity. *J Mater Process Technol* 211(10):1590–1598
41. Ulutan D, Ozel T (2011) Machining induced surface integrity in titanium and nickel alloys: a review. *Int J Mach Tools Manuf* 51(3):250–280
42. Bezerra MA, Santelli RE, Oliveira EP, Villar LS, Escaleira LA (2008) Response surface methodology (RSM) as a tool for optimization in analytical chemistry. *Talanta* 76(5):965–977
43. Sahu NK, Andhare AB (2017) Modelling and multiobjective optimization for productivity improvement in high speed milling of Ti–6Al–4V using RSM and GA. *J Braz Soc Mech Sci Eng*. 10.1007/s40430-017-0804-y
44. Gaitonde VN, Karnik SR, Davim JP (2009) Multiperformance optimization in turning of free-machining steel using Taguchi method and utility concept. *J Mater Eng Perform* 18(3):231–236
45. Wan Y, Cheng K, Liu Z, Ye H (2013) An investigation on machinability assessment of difficult-to-cut materials based on radar charts. *Proc Inst Mech Eng Part B J Eng Manuf* 227(12):1916–1920. <https://doi.org/10.1177/0954405413497008>